Invited Paper

# Requirements for MEMS Mirrors for Adaptive Optics in the Eye

Elizabeth Daly, Eugenie Dalimier and Chris Dainty

Applied Optics Group, Department of Experimental Physics,
National University of Ireland, Galway, Ireland.

## ABSTRACT

MEMS is one of several emerging technologies for fabricating wavefront correctors for use in adaptive optics systems. Each technology has its own advantages and disadvantages. In order to compare devices, it is useful to define a task and make a comparison based upon the effectiveness of each device for this task. Such an approach implies, of course, that device A might be better suited for task X whereas device B is better suited for task Y. In adaptive optics, this situation is already known: deformable mirrors that are relatively effective at compensating for atmospheric turbulence are not necessarily the mirrors that one would choose for correction of the aberrations of the eye. This is essentially because the statistical modal distribution of the aberrated wavefronts in each case are different. In this talk, we shall present a method for systematically evaluating the effectiveness of different mirror (or transmissive) technologies in adaptive optics in the eye. It uses a model for the aberrations of the eye (such as that developed by Thibos et al[1]) and a least squares fitting procedure. Results will be presented for at least 4 mirrors, including a 12x12 MEMS device. The key point is that it is the effectiveness of each actuator signal that is important, not the raw number of actuators.

**Keywords:** Deformable mirror, MEMS, adaptive optics, vision science

## 1. INTRODUCTION

There are now many different types of deformable mirrors available commercially, employing different technologies, having different numbers and arrangements of actuators, and capable of different strokes. Most have been used successfully in a variety of adaptive optics (AO) experiments. The first wavefront correctors developed were segmented, and were used to correct for the aberrations introduced by the atmosphere. The small gaps between the discrete segments however, lead to energy losses and wavefront fitting errors, so that segmented mirrors have been mostly superseded by continuous facesheet correctors which can apply a smooth correction to the wavefront. For example, the properties of high-power laser beams and pulses have been modified with bulk micromachined membrane mirrors[2,3] and bimorph devices.[4] The aberrations of the human eye were first corrected by Liang et al[5] in 1997 using a DM based on piezoelectric technology. Other devices used in vision science include membrane,[6] micromechanical[7] and bimorph[8] mirrors, and liquid crystal spatial light modulators.[9]

In adaptive optics (AO) the *best* DM to use depends not only on the properties of the DM, but also on the structure of the wavefront aberrations to be corrected. The problem in vision science is that ocular aberrations are not as well characterized statistically as those introduced by atmospheric turbulence. The dimensions of the system to be corrected are also important: it is easier to build a compact system for vision science if the DM used has similar dimensions to the pupil of the eye. Using a large DM requires more use of relay optics leading to a larger instrument. On the other hand, larger mirrors are desirable in atmospheric AO as one is conjugating to the entrance pupil of a telescope.

How does one choose the best DM for a particular application? Here we build on a previous study[10] in which we define a task and assess the suitability of four different DMs to perform that task. The task is correction of

Further author information: (Send correspondence to C.D.)
E.D.: E-mail: elizabeth.daly@nuigalway.ie, Telephone: +353 (0)91 492985
Eu.D.: E-mail: eugenie.dalimier@nuigalway.ie, Telephone: +353 (0)91 495191
C.D.: E-mail: c.dainty@nuigalway.ie, Telephone: +353 (0)91 512374

MEMS/MOEMS Components and Their Applications III,
edited by Scot S. Olivier, Srinivas A. Tadigadapa, Albert K. Henning,
Proc. of SPIE Vol. 6113, 611309, (2006) · 0277-786X/06/$15 · doi: 10.1117/12.653409

the aberrations in healthy human eyes. We use a statistical model for the aberrations developed by Thibos *et al.*[1] to produce typical ocular wavefronts. We also look at the ability of the DMs to generate Zernike modes, as ocular wave fronts are usually expressed in terms of these polynomials.

## 2. DEFORMABLE MIRRORS

Of the four devices characterised here, three were described in detail previously.[10] They are:

- A 37-channel bulk micro-machined membrane mirror from Flexible Optical BV. This device has a total stroke of about 3.5 $\mu$m peak-to-valley with individual actuators capable of 500 nm.
- A 19-channel piezoelectric device from the same supplier. The stroke of this device is larger than the membrane mirror partly because the edge of the mirror is free to move; we measured 3 $\mu$m stroke for the central actuators and 7-9 $\mu$m for the outer actuators for the voltage range used. A complication of this device when used in a closed-loop AO system is the relatively large degree of hysteresis - about 14% of total deformation.
- A 35-channel AOptix mirror with 16 $\mu$m of total stroke and individual actuator strokes similar to the 19-channel device. The inner actuators produce a curvature deformation while the outer ones generate slopes.

In this work we add the the results obtained from a surface micromachined microelectromechanical (MEMS) mirror produced by Boston Micromachines (BMC) Inc.[11] An array of parallel-plate electrostatic actuators is coupled to a continuous mirror membrane by mechanical posts. The 140 actuators are arranged in a 12x12 square matrix with approximately 400 $\mu$m spacing between the actuator centers. The active area of the mirror is 3.3 x 3.3mm, an excellent match to the typical pupil size of the human eye. At the maximum drive voltage of 275V, the stroke of the mirror was measured to be 3.5 $\mu$m. We found that the deflection produced by a single actuator followed a V-squared dependence on voltage as did that produced by a 2x2 array, but for an array of 9 actuators or more, the deflection of the mirror was linear with respect to voltage. The actuators were numbered in concentric squares, so that actuators 1-4 are in the center of the mirror, 5-16 in the next "ring" (rectangular), 17-36 outside that etc.

**Table 1.** Deformable mirrors tested

| **Mirror** | **Technology** | **Diameter (mm)** | **Actuators** | **Stroke ($\mu$m)** |
|---|---|---|---|---|
| OKO37 | Electrostatic | 15 | 37 | 3.5 |
| OKO19 | Piezoelectric | 30 | 19 | 3, 7-9 |
| AOptix35 | Electrorestrictive | 10.2 | 35 | 16 |
| BMC140 | Electrostatic | 3.3 x 3.3 | 140 | 3.5 |

The main properties of the deformable mirrors tested here are summarized in Table 1, and the arrangement of actuators and typical pupil sizes used in the measurements are shown in Figure 1.

## 3. PHASE FITTING PROCEDURE

The response of a DM to the application of voltages to its actuators is called the Influence Function Matrix (IFM). This matrix contains all the information to characterize the DM spatially as it relates each unit of applied voltage $v$ to a resulting phase map $\phi$

$$\phi = \mathbf{IFM}v. \tag{1}$$

The influence functions for each DM were measured with a commercial FISBA Twyman Green interferometer, with the result for each actuator taken as the difference between two phase measurements, one either side of the

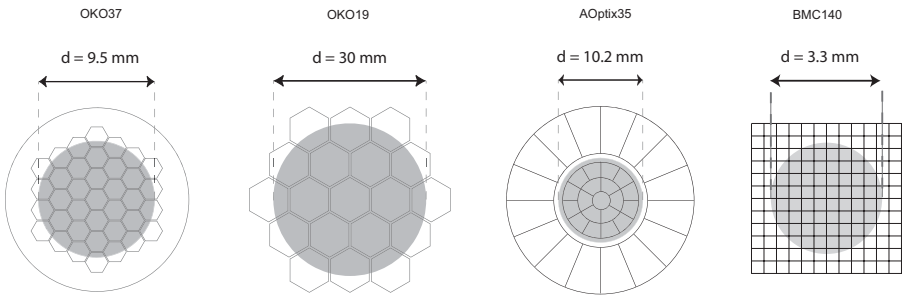


**Figure 1.** Actuator layout of mirrors tested, with the typical pupil size shown shaded.

mid or bias position. All influence functions were normalized to the range of voltages used in the calibration, and the piston terms were removed. For wave-front correction, the inverse of Eq. 1 is required: on measuring a wavefront $\phi$, what control voltages are required to cancel that wavefront shape

$$v = \mathbf{IFM}^{-1}\phi? \tag{2}$$

However, because the inverse of the IFM is not generally available, the technique of Singular Value Decomposition (SVD) is often used to write it as a product of terms which can be inverted

$$\mathbf{IFM} = \mathbf{UWV}^T. \tag{3}$$

Here, $\mathbf{U}$ and $\mathbf{V}$ are matrices with orthogonal columns and $\mathbf{W}$ is a diagonal matrix containing the singular values. $\mathbf{U}$ represents the spatial modes of the mirror and $\mathbf{V}$ represents the mirror control commands that are related to these modes through the singular values. The mirror is capable of producing any wavefront shape that can be expressed as a linear combination of the orthogonal modes. A small singular value means that the related mode has a large system gain and is susceptible to noise, but with SVD these modes can be filtered out by setting their singular values equal to zero in the pseudoinverse.

In this study we simulated the capability of each mirror to generate certain phase maps - the raw Zernike modes and typical ocular wavefronts generated with the Thibos model. Any phase $\phi$ can be projected onto the mirror basis set through

$$\phi_M = \mathbf{U}\mathbf{U}^T\phi \tag{4}$$

where the fitting error for each mirror was taken as the root mean square (RMS) of the difference between the two wavefronts - $\phi$ and $\phi_M$. The mirror commands required to generate $\phi$ were calculated from Eq. 2 using the SVD of IFM to enable calculation of its psuedoinverse

$$v = \mathbf{IFM}^{-1}\phi = \mathbf{VW}^{-1}\mathbf{U}^T\phi. \tag{5}$$

In a real experiment the allowed voltage commands are limited to some range, and this must be reflected in the simulation.

## 4. SIMULATION RESULTS

### 4.1. Characteristics of the MEMS mirror

As the performance of the first three mirrors was discussed in detail in our previous study, here we will concentrate on the MEMS device and how it compares to the others. The largest pupil used in the characterization of this mirror was 3.3 mm, which is equal to the active area of the mirror. With this pupil, it was possible to see an effect from all but the outer ring of actuators and some in the corners of the inner rings. Apart from these actuators, the PV of the influence functions measured across the mirror diameter are very similar (approximately 1 $\mu$m PV for the voltage range used in the calibration). They are also quite localized compared to those obtained with, for example, the 37-channel membrane mirror, having a full width at half maximum (FWHM) of just 550 $\mu$m.

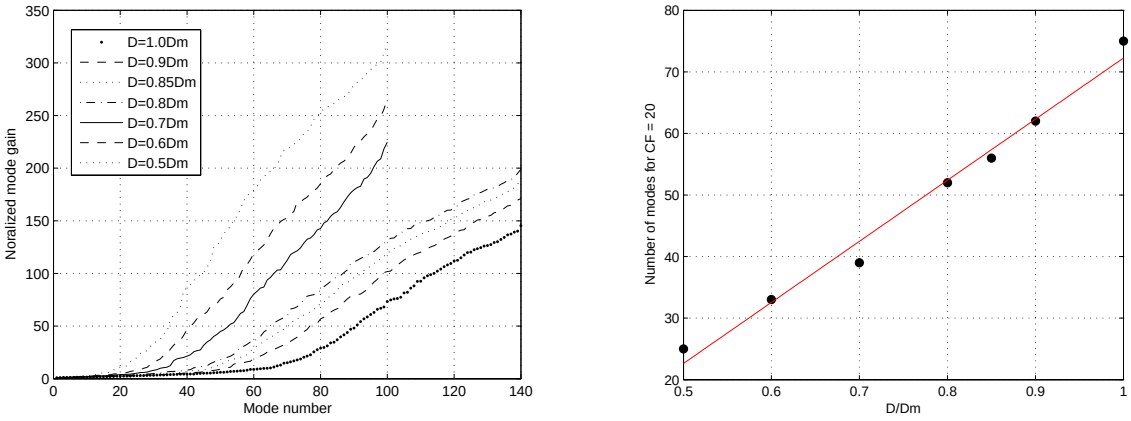


**Figure 2.** BMC mirror normalized mode gains as a function of pupil size at the mirror, and number of modes required for condition factor of 20. The solid line is a linear fit to the data.

The gain of the MEMS mirror modes as a function of fraction of active area probed $D/D_m$ are shown in Figure 2. Regardless of the area used, we found that there are two regimes with different rates of increase. We also found that the number of mirror modes at which the gain reaches a value of 20 increases linearly with $D/D_m$. This cutoff point corresponds to an informal rule of thumb to disregard modes with singular values smaller than 0.05 (condition factor greater than 20) in order to make the mirror control more robust.

### 4.2. Fitting Zernike modes.

A first indication of the capabilities of each mirror was obtained by simulating how well each could generate Zernike polynomials, ordered according to the OSA/VSIA Taskforce conventions.[12] $Z_M = UU^T Z$ was calculated where $Z$ is the set of normalized ideal Zernikes and $Z_M$ are those produced by the mirror. The command voltages for each mode were then re-scaled to account for the maximum per mode and to cover half of the allowed voltage range. In this way the $Z_M$ calculated corresponds to a maximum signed quantity, i.e. the mirror is capable of producing $\pm Z_M$ of wavefront deformation. The maximum PV of the Zernike term produced by each mirror is shown in Figure 3. In terms of raw stroke the AOptix mirror and the 19-channel piezo device perform very well and have comparable capabilities. It is interesting to note that although the 37-channel membrane mirror and

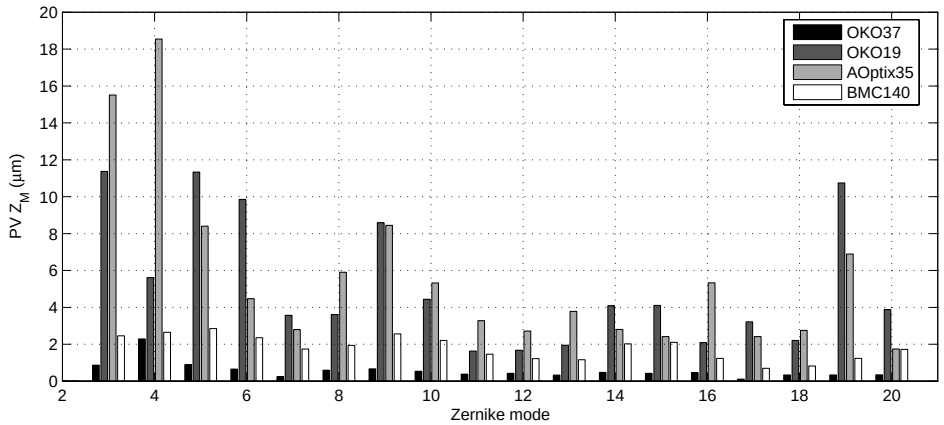


**Figure 3.** Maximum PV of signed $Z_M$.

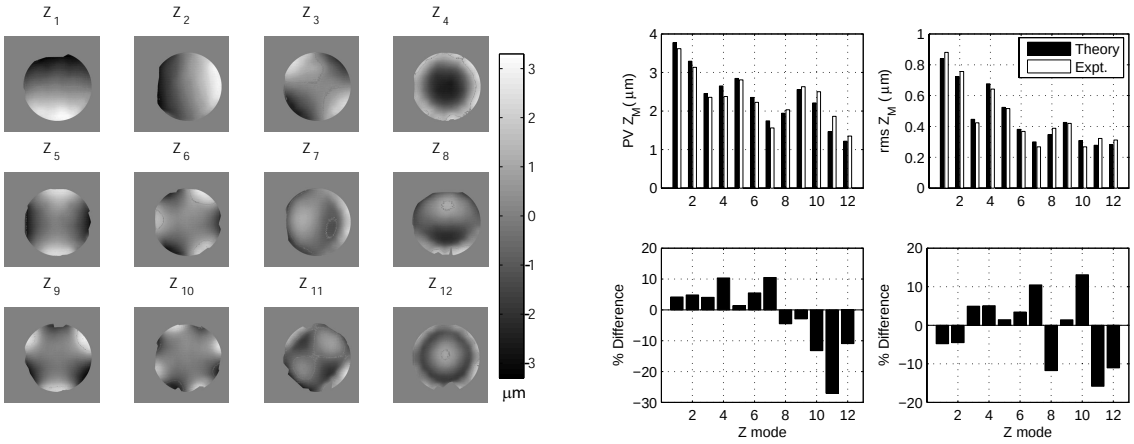


**Figure 4.** Experimental Zernike modes measured for BMC140 mirror and comparison of measured PV and RMS values with theory. These measurements were taken using the full active area of the mirror, 3.3 mm diameter. The faint contour lines visible in some modes show regions where the phase passes through zero.

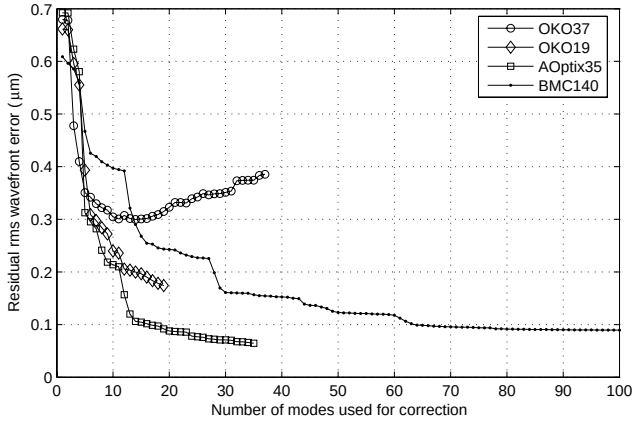


**Figure 5.** Residual rms wavefront error after fitting with the four mirrors to the same initial ocular wavefront.

the MEMS mirror have the same stroke, the MEMS mirror is far superior in terms of PV deformation and fitting error. The greater number of actuators on the MEMS device appears to have a very positive effect here. In general, the results obtained for the 37-channel membrane and 35-channel bimorph mirrors are consistent with similar studies by Fernández *et al.*[13] and Horsley *et al.*[14] on these devices.

The voltage commands necessary to generate the first twelve Zernike modes were applied to the MEMS mirror and the resulting phase maps were measured using the FISBA interferometer. The results are shown in Figure 4. There is excellent agreement between experiment and the theory, as also shown in this figure. In the interests of speed the wavefronts shown were obtained on application of the required voltage commands to actuators 1-100 only, while the remaining actuators were maintained at the bias position. We found negligible difference in the measured PV and RMS of the resulting wavefronts on including this outer ring of actuators.

### 4.3. Fitting typical ocular wavefronts.

Fitting Zernike modes with each DM is a useful step to compare their potential to generate any wavefront. However wavefront reconstruction with the Zernike polynomials is not an automatic step in most adaptive optics

experiments; for one thing it slows down operation of the loop. It is arguably more accurate to simulate how well a mirror can fit a specific wavefront which is representative of the aberrations to be corrected. The problem for AO in vision science is that ocular aberrations cannot be described by any simple model, for example in the way that Kolmogorov theory can describe the aberrations caused by the atmosphere. The best so far that one can do is to look at the statistics of the aberrations as measured experimentally for large numbers of eyes. Here we generate typical ocular wavefronts based on experimental studies of healthy well-corrected (astigmatism and defocus) eyes by Thibos *et al.*.[1,12] Eq. 5 was used to calculate the commands required to generate the sample wavefront, which were inserted into Eg. 1 to calculate the ocular wavefronts that the mirror was capable of producing. The SVD of the IFM was used in both cases. Commands which were found to be out of range were clipped at the maximum or minimum allowed, leading to small differences between the sample wavefront and the mirror's representation of it - this leads to a fitting error. The target wavefronts were samples of 100 eyes generated over 6 mm ocular pupils. The residual rms error after fitting to the same initial wavefront with each of the mirrors as a function of the number of modes used is shown in Figure 5. As noted in our previous study,[10] there is evidence of actuator saturation due to inclusion of "noisy" modes for the OKO37 mirror. On the other hand, the large-stoke AOptix35 bimorph mirror performs better as more modes are used. This is also the trend for the OKO19 piezo mirror, although the small number of actuators means that performance is not as good overall. The fitting error for the BMC140 MEMS mirror also decreases as more modes are included in the calculation, although we found only negligible improvements on using more than 100 modes here. The minimum residual error is attained more gradually for this mirror, probably a result of the relatively localized influence functions. It is interesting to compare the OKO37 and BMC140 mirrors as they have practically identical strokes. They do however differ in the number and arrangement of actuators, and this leads to very different results in terms of correcting the aberrations of the eye as simulated here. These results would lead us to conclude that it is the effectiveness of each actuator signal that is important, not the raw number of actuators.

We also investigated the performance of the BMC140 mirror as a function of the beam diameter, $D/D_m$, where $D_m$ is 3.3 mm. We found that the lowest residual error was achieved on using the full diameter, and that it increased as less of the mirror was used. These results are shown in Figure 6. What is interesting is that the optimum number of modes to use for fitting does show some differences depending on the beam diameter at the mirror. This is illustrated in Figure 7, where the difference in residual rms error obtained on using some fraction of the mirror rather than its full active area is plotted. Each curve on this graph was obtained by subtracting the residual rms error obtained on using the full mirror diameter from that obtained on using some fraction. This means that the curve corresponding to $D_m$ is zero because it is the difference of two identical quantities for each number of modes. Values greater than zero mean that using that fraction $D/D_m$ of the mirror results in a higher residual than using the full mirror; values less than zero mean that the residual is reduced on using less

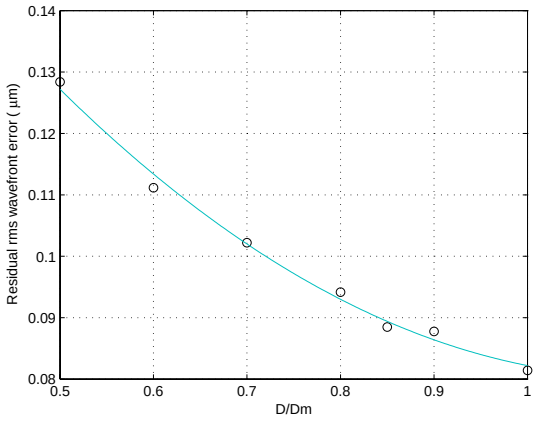


**Figure 6.** Final residual rms wavefront error as a function of $D/D_m$ on fitting with 100 modes of the BMC140 mirror. The line is a quadratic fit to the data.

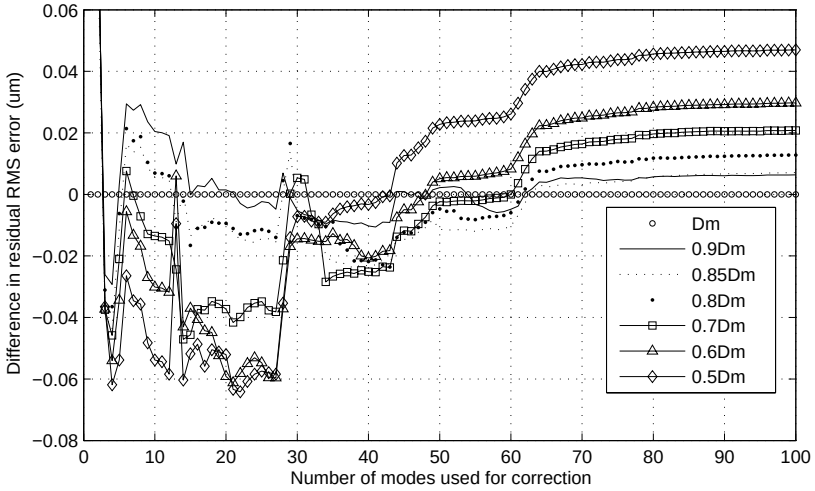


**Figure 7.** Differences in residual RMS wavefront error for the BMC mirror as a function of mirror diameter used.

than the full diameter. In general it would seem that if one is only going to use 10 - 30 modes for correction, then the best results will occur on using less than the full diameter. If the number of modes to be used is greater than about 60, then the best fitting will be achieved with the full active area of the mirror.

## 5. CONCLUSION

We have simulated the ability of four different commercially-available deformable mirrors to fit typical ocular wavefronts. Only static aberrations are considered, and it is assumed that the actuator influence functions add in a linear fashion. The best performance was achieved with a 35-actuator bimorph deformable mirror, which had the largest stroke of all the mirrors tested. The MEMS device performed second best, despite having less or equal stroke than the two remaining mirrors. On the other hand it does have far more actuators than the other devices, so that it performs much better than, for example, the OKO37 device which has exactly the same stroke. What these calculations show is that it is *both* the raw number of actuators and the arrangement and effectiveness of each individual actuator which determine how well a mirror will perform a particular task. The best mirror to use for ocular adaptive optics may well be a combination of two devices as suggested by Horsley *et al.*[14] - a large-stroke mirror with few actuators to correct for low-order modes, and a modest-stroke mirror with lots of actuators to look after the high-order aberrations.

## ACKNOWLEDGMENTS

We are grateful to Larry Thibos who provided us with his MATLAB files for the ocuclar aberration statistics and the functions to randomly generate a standard-eye wavefront.

This research is funded by Science Foundation Ireland under Grant No. SFI/01/PI.2/B039C and by a European Union EU Research Training Network, contract number HPRN-CT-2002-00301 "SHARP-EYE".

## REFERENCES

1. L. Thibos, A. Bradley, and X. Hong, "A statistical model of the aberration structure of normal, well-corrected eyes," *Ophthal. Physiol. Opt.* **22**, pp. 427–433, 2002.
2. W. Lubeigt, G. Valentine, J. Girkin, E. Bente, and D. Burns, "Active trasverse mode control and optimisation of an all-solid-state laser using an intracavity adaptive-optic mirror," *Opt. Exp.* **10**, pp. 550–555, 2002.

3. E. Zeek, K. Maginnis, S. Backus, U. Russek, M. Murnane, G. Mourou, H. Kapteyn, and G. Vdovin, "Active trasverse mode control and optimisation of an all-solid-state laser using an intracavity adaptive-optic mirror," *Opt. Lett.* **24**, pp. 493–495, 1999.
4. T. Y. Cherezova, L. N. Kaptsov, and A. V. Kudryashov, "Cw industrial rod yag:nd3+ laser with an intracavity active bimorph mirror," *Appl. Opt.* **35**, pp. 2554–2561, 1996.
5. J. Liang, D. R. Williams, and D. Miller, "Supernormal vision and high-resolution retinal imaging through adaptive optics," *J. Opt. Soc. Am. A* **14**, pp. 2884–2892, 1997.
6. E. J. Fernández, I. Iglesias, and P. Artal, "Closed-loop adaptive optics in the human eye," *Opt. Lett.* **26**, pp. 746–748, 2001.
7. N. Doble, G. Yoon, L. Chen, P. Bierden, B. Singer, S. Olivier, and D. R. Williams, "Use of a microelectromechanical mirror for adaptive optics in the human eye," *Opt. Lett.* **27**, pp. 1537–1539, 2002.
8. M. Glanc, E. Gendron, F. Lacombe, D. Lafaille, J.-F. L. Gargasson, and P. Léna, "Towards wide-field retinal imaging with adaptive optics," *Opt. Comm.* **230**, pp. 225–238, 2004.
9. F. Vargas-Martín, P. M. Prieto, and P. Artal, "Correction of the aberrations in the human eye with a liquid-crystal spatial light modulator: limits to performance," *J. Opt. Soc. Am. A* **15**, pp. 2552–2562, 1998.
10. E. Dalimier and C. Dainty, "Comparative analysis of deformable mirrors for ocular adaptive optics," *Opt. Exp.* **13**, pp. 4275–4285, 2005.
11. T. G. Bifano, J. Perreault, R. Krishnamoorthy, and M. N. Horenstein, "Microelectromechanical deformable mirrors," *IEEE J. Sel. Top. Quant. Electron.* **5**, pp. 83–89, 1999.
12. L. Thibos, R. A. Applegate, J. T. Schwiegerling, and R. Webb, "Standards for reporting optical aberrations of eyes," *J. Refract. Surg.* **18**, pp. 652–660, 2000.
13. E. J. Fernández and P. Artal, "Membrane deformable mirror for adaptive optics: performance limits in visual optics," *Opt. Exp.* **11**, pp. 1056–1069, 2003.
14. D. A. Horsley, H. Park, S. P. Laut, and J. S. Werner, "Characterization for vision science applications of a bimorph deformable mirror using phase-shifting interferometry," in *Ophthalmic Technologies XV*, F. Manns, P. G. Sderberg, A. Ho, B. E. Stuck, and M. Belkin, eds., *Proc. SPIE* **5688**, pp. 133–144, 2005.